Rheological properties and engineering application of low-grade asphalt mixture

Liang Song[1,2,3], Pengcheng Tu[4], Xiaodong Xie[4,5], Jingjing Fan[4], Lulu Hou[4], Jie Gao[6]

[1]Xinjiang Transportation Investment (Group) Co., Ltd. 830006, Urumqi China.

[2]Xinjiang Communications Investment Construction Management Co., Ltd. 830099, Urumqi, China.

[3]Key Laboratory of China's Transportation Industry for Highway Engineering Technology in Arid Desert Region. 830099, Urumqi, China.

[4]Xinjiang Agricultural University, School of Transportation and Logistics. 830091, Urumqi, China.

[5]Xinjiang Vocational and Technical College of Communications. 831401, Urumqi, China.

[6]East China Jiaotong University, School of Civil Engineering and Architecture. 330013, Nanchang, China.

e-mail: slpl@sohu.com, 320212738@xjau.edu.cn, xiaodong3056@163.com, 320222569@xjau.edu.cn, luluya1868@163.com, gaojie@ecjtu.edu.cn

ABSTRACT

This study investigates the feasibility of low-grade hard asphalt in high-temperature regions. We conducted an analysis of the high-temperature rheological properties of asphalt before and after short-term and long-term aging using the dynamic shear rheological (DSR) test and multi-stress creep recovery (MSCR) test. Additionally, the road performance of the asphalt mixture was studied by rutting test and low temperature beam bending test. The results indicate that the 30# asphalt demonstrates superior anti-rutting performance compared to the 50# asphalt. Furthermore, the rutting factor and fatigue factor of the 30# asphalt during aging are significantly higher than those of the 50# asphalt. With increasing temperature, stress level, and stress action time, the strain of the asphalt gradually increases. The unrecoverable creep compliance of the 50# asphalt exceeds that of the 30#. Although the high-temperature performance of the 30# asphalt mixture outperforms that of the 50# asphalt mixture, it exhibits lower flexural tensile strength and deformation ability at low temperatures compared to the 50# asphalt mixture. Overall, low-grade asphalt demonstrates relatively stable stress variations and exhibits good high-temperature stability.

Keywords: Low-grade hard asphalt; Aging; High-temperature rheological properties; Road performance.

1. INTRODUCTION

Low-grade hard asphalt exhibits characteristics such as low penetration, high rigidity, and high hardness [1].

Low-grade asphalt mixture refers to asphalt with high permeability and low viscosity, typically exhibiting permeability within the range of 40–80 dmm. Low-grade asphalt is characterized by low penetration, high rigidity, and high hardness [1]. France initiated research on low-grade hard asphalt as early as the 1960s, leading to significant advancements [2, 3]. In the early 21st century, the specification included the use of high modulus asphalt mixture prepared with hard asphalt.

Numerous studies have demonstrated that low-grade asphalt mixtures exhibit favorable rheological properties at elevated temperatures [4, 5]. The low viscosity of low-grade asphalt mixtures facilitates the formation of a dense asphalt film at high temperatures, thereby enhancing pavement shear and deformation resistance. NASCIMETO *et al.* [6] focused on hard asphalt mixtures as their primary research subject and assessed them using the Hamburg rutting test, which revealed excellent resistance to high-temperature deformation.

To investigate the deformation and flow of asphalt under external forces, rheological parameters are commonly employed to assess asphalt pavement performance [7] and analyze the impact of aging on asphalt material rheological properties [8, 9]. The high-temperature rheological properties of asphalt are studied using Dynamic Shear Rheometer (DSR) tests, and the rutting factor (G* / sinδ) is employed to evaluate its high-temperature performance [10, 11]. Additionally, the Multi-Stress Creep Recovery (MSCR) test has been suggested by some

researchers as an effective method to assess the rheological properties of asphalt, where the high-temperature performance is evaluated based on creep recovery rate and non-recoverable creep compliance [12, 13].

Under high-temperature conditions, low-grade asphalt mixture exhibits excellent performance and stability, making it suitable for use in road construction in hot regions. However, JUDYCKI *et al.* [14] and KOMARAGIRI *et al.* [15] found that hard asphalt performs poorly at low temperatures compared to regular asphalt. ESPERSSON [16] conducted experiments on hard asphalt at various temperatures and observed that the modulus and viscosity of hard asphalt mixture were higher at lower temperatures. In summary, low-grade hard asphalt offers advantages such as rutting resistance, reduced pavement stiffness, and material savings. It can serve as an effective combination for high-modulus asphalt mixtures and long-life asphalt pavements [17, 18]. However, further investigation is required to determine the low-temperature performance of low-grade asphalt mixtures.

Over time and under changing environmental conditions, asphalt undergoes an inevitable aging process, resulting in a gradual decline in performance [19, 20]. As the use of low-grade asphalt in asphalt mixtures is relatively recent, research on its aging performance remains limited. Various factors, such as temperature, oxygen, ultraviolet radiation, humidity, and vehicle load [21, 22], influence the aging of asphalt, leading to the fracture of asphalt molecular chains, oxidation reactions, and changes in chemical composition, consequently altering the physical and chemical properties of asphalt [23, 24]. Additionally, asphalt aging affects its adhesion to aggregates and interactions with the environment, thereby impacting road stability and durability [25, 26]. Compared to high-grade asphalt, low-grade hard asphalt may exhibit different behaviors and performance changes during aging, necessitating comprehensive research.

In terms of engineering applications, low-grade asphalt mixtures have found extensive use in road construction, especially in high-temperature areas. According to MITTAL *et al.* [27], experimental analysis demonstrated that the application of new hard asphalt can reduce the thickness of the dense asphalt gravel layer, resulting in significant savings in materials and funds. Moreover, the cost of low-grade asphalt mixtures is relatively low, making them economically feasible for large-scale road construction projects.

This paper focuses on investigating the rheological properties of 30# and 50# low-grade virgin asphalt under various temperatures and aging conditions using dynamic shear rheometer (DSR) and multiple stress creep recovery test (MSCR). Additionally, it examines the performance of low-grade asphalt mixtures. The findings offer valuable suggestions and technical support for the practical implementation of low-grade asphalt in high-temperature areas.

2. MATERIALS AND METHODS

2.1. Materials

2.1.1. Asphalt

The study selected Karamay 30 # and 50 # asphalt produced locally in Xinjiang, and the asphalt technical indicators are shown in Table 1.

2.1.2. Aggregate

The aggregate is limestone, and the mineral powder is ground limestone powder. The test results of aggregate properties are shown in Table 2.

2.1.3. Gradation

The mineral aggregate used in this study followed the gradation range based on the median value of AC-25 gradation. By optimizing the sieve content, a new AC-25 gradation design curve was developed. The resulting

Table 1: Low-grade asphalt technical indicators.

ASPHALT	(25 °C, 100g, 5s) PENETRATION (0.1 mm)	SOFTENING POINT (°C)	(5cm · min^{-1}, 5 °C) DUCTILITY (cm)	135 °C DYNAMIC VISCOSITY (Pa · S)
30#	26	57.4	22.5	1064.32
50#	43.9	53.3	>100	353.6

Table 2: Aggregate technical indicators.

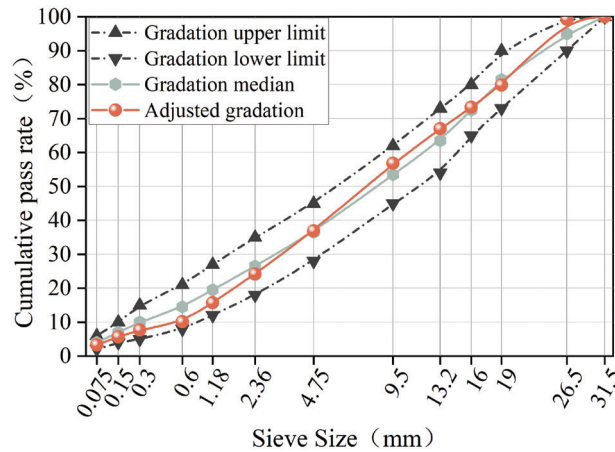| TESTING ITEMS	PARTICLE SIZE (mm)	TEST VALUE	TECHNICAL REQUIREMENTS
Crush value (%)	9.5–13.2	14.64	≤26
	4.75–9.5	6.73	≤18
	9.5–16	7.91	≤12
Needle flake particle content (%)	16–19	5.40	≤12
	19–26.5	7.13	≤12

Figure 1: AC-13C coarse dense grading.

synthetic gradation curve is presented in Figure 1. The optimum asphalt content for the 30# and 50# low-grade asphalt mixtures was determined through the Marshall test to be 4.07% and 4.10%, respectively.

2.2. Test methods

2.2.1. Thermal-oxidative aging

The short-term aging of the asphalt samples was conducted using the rotating thin film oven test (RTFOT). A clean aging bottle was prepared for this purpose. Approximately 35g ± 0.5g of the original asphalt was loaded into the bottle and allowed to cool to room temperature. The aging bottle was then inserted into each hole of the oven ring frame, and the flow meter was adjusted to maintain an air flow rate of 4000 mL/min ± 200 mL/min. The aging bottle was subjected to continuous heating at a temperature of 163.0 ± 0.5 °C for a duration of 85 minutes. Subsequently, the sample was quickly poured into a pre-prepared container to obtain the short-term aged asphalt sample.

The long-term aging Pressure Aging Vessel (PAV) test was conducted on the samples after the RTFOT test. The test utilized the Prentex 9500 PAV pressure aging container manufactured by Euro-American Land Company. The instrument was first opened and preheated to 100 °C. Meanwhile, approximately 50 ± 0.5g of the residue from the RTFOT test was weighed and loaded into the aging sample tray, which was then placed on the designated sample rack. Once the temperature reached 100 °C, the sample holder was placed inside the pressure vessel, and the vessel was sealed. The temperature was allowed to stabilize at around 99 °C, and then air pressure of 2.1 MPa ± 0.1 MPa was supplied for a duration of 20 hours. If the temperature during the aging process fell below 99.5 °C or exceeded 100.5 °C, and the duration exceeded 60 minutes, the aging test was considered unsuccessful.

2.2.2. DSR test

DSR tests were conducted on 30# and 50# asphalt samples before and after aging at various temperatures using a dynamic shear rheometer manufactured by TA Instruments, an American company. The fixed loading frequency was set at 10 rad/s, and the test temperature range spanned from 52 °C to 82 °C, with each test interval being 6 °C. The DSR test employed a parallel plate configuration with a diameter of 25 mm and a gap of 1 mm

between the upper and lower plates. The test measured the complex modulus G*, phase angle δ, and rutting factor G* / sinδ of the low-grade asphalt before and after aging.

2.2.3. MSCR test

The MSCR (Multiple Stress Creep Recovery) test of asphalt was conducted using a dynamic shear rheometer. The test involved subjecting the asphalt sample to loading and unloading cycles. The MSCR test consisted of two stages. In the first stage, the asphalt sample was subjected to a creep phase of 1 second followed by a recovery deformation phase of 9 seconds, under a stress condition of 0.1 kPa. This cycle was repeated 10 times. In the second stage, the asphalt sample was subjected to a creep phase of 1 second followed by a recovery deformation phase of 9 seconds, under a stress condition of 3.2 kPa. This cycle was also repeated 10 times. The test temperatures for the MSCR test were 52 °C, 64 °C, 72 °C, and 82 °C.

The test index R and the calculation process of J_{nr} are as Equations (1) and (2), where ε_0 is the strain measured at the beginning of creep, ε_c is the strain measured at the end of creep, and ε_r is the strain value at the end of the recovery part of a single cycle.

$$J_{nr}(\sigma, N) = \frac{\varepsilon_r - \varepsilon_0}{\sigma} \tag{1}$$

$$R(\sigma, N) = \frac{\varepsilon_c - \varepsilon_r}{\varepsilon_c - \varepsilon_0} \times 100 \tag{2}$$

Where: σ is the applied stress, kPa; n is the number of creep and cycles; $J_{nr}(\sigma, N)$ is the unrecoverable creep compliance measured under a given cycle, kPa^{-1}; $R(\sigma, N)$ is the creep recovery rate measured under a given cycle, %.

The evaluation indexes used in this paper are $R_{0.1}$, $R_{3.2}$, $J_{0.1}$, $J_{3.2}$, respectively, the average value of creep recovery rate under 0.1 kPa stress, the average value of creep recovery rate under 3.2 kPa stress, the average value of unrecoverable creep compliance under 0.1 kPa stress, and the average value of unrecoverable creep compliance under 3.2 kPa stress, as shown in Equations (3) to (6).

$$R_{0.1} = \frac{SUM[\varepsilon_r(0.1, N)]}{10} \tag{3}$$

$$R_{3.2} = \frac{SUM[\varepsilon_r(3.2, N)]}{10} \tag{4}$$

$$J_{nr0.1} = \frac{SUM[J_{nr}(0.1, N)]}{10} \tag{5}$$

$$J_{nr3.2} = \frac{SUM[J_{nr}(3.2, N)]}{10} \tag{6}$$

The relative difference of unrecoverable creep compliance $J_{nr\,diff}$ and the relative difference of creep recovery rate R_{diff} are calculated by Equations (7) and (8).

$$J_{nrdiff} = \frac{[J_{nr3.2} - J_{nr0.1}]}{J_{nr0.1}} \times 100 \tag{7}$$

$$R_{diff} = \frac{[R_{0.1} - R_{3.2}]}{R_{0.1}} \times 100 \tag{8}$$

2.2.4. Rutting test

First, rut plate specimens measuring 300 mm × 300 mm × 50 mm were prepared by wheel rolling at a temperature of 25 °C. These specimens were then allowed to rest at room temperature for 48 hours to stabilize. Next, the specimens were placed inside an environmental box set at a temperature of 60 °C ± 1 °C for a duration of 6 hours. Following the conditioning period, the rut test was conducted using a rut tester. The test wheel was positioned at the center of the specimen, and the test temperature was maintained at 60 ± 0.5 °C. The test wheel traversed back and forth over the specimen for a total duration of 1 hour. The deformation curve and specimen temperature were continuously recorded by an automated rut deformation recorder throughout the test.

2.2.5. Low temperature beam bending test

The rutting plate is trimmed after being removed from the mold to obtain a prismatic trabecular specimen with dimensions of 250 mm × 30 mm × 35 mm. A UTM (Universal Testing Machine) pavement material testing machine was utilized for single-point loading, with a loading rate of 50 mm/min. The testing temperature was maintained at –10 °C. During the experiment, the force-displacement curve was recorded to determine the flexural tensile strength at failure, the maximum flexural tensile strain at the bottom of the beam after failure, and the flexural stiffness modulus at failure.

3. RHEOLOGICAL PROPERTIES OF LOW-GRADE ASPHALT

3.1. High temperature viscoelastic analysis of asphalt based on temperature scanning

3.1.1. Complex shear modulus

The complex modulus G* is an indicator of asphalt's resistance to deformation. A higher value indicates a stronger ability to resist deformation. Figure 2 presents the complex modulus curves of 30# and 50# low-grade asphalt before and after aging, specifically focusing on warm mix asphalt with temperature variations. The graph demonstrates a decreasing trend in G* as temperature increases, indicating a reduction in asphalt's deformation resistance with rising temperature. Both types of asphalt exhibit similar decreasing trends in complex shear modulus, characterized by an initial rapid decline followed by a slower decrease, eventually reaching a stable state. The rate of decline in the temperature range of 52 °C to 70 °C is higher than that in the range of 70 °C to 82 °C. This can be attributed to the diminished anti-deformation capability of asphalt at higher temperatures, leading to a decrease in deformation rate once a certain threshold is reached. Notably, after aging, the complex shear modulus of both types of asphalt shows a significant increase. A comparison between the aging methods of RTFOT and PAV reveals that PAV aging exerts the greatest influence on asphalt, resulting in the highest resistance to dynamic shear deformation among the two aging methods.

3.1.2. Phase angle

The phase angle δ provides insight into the balance between the viscous and elastic components of asphalt binder. A larger δ indicates a higher proportion of the viscous component, resulting in a weaker recovery deformation
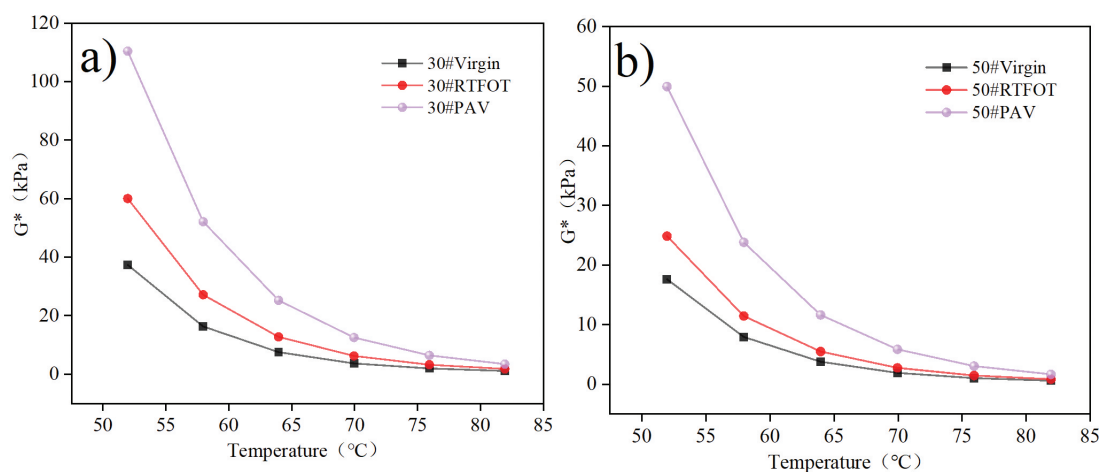

Figure 2: Complex shear modulus under different aging conditions and different temperatures: (a) 30# asphalt; (b) 50# asphalt.
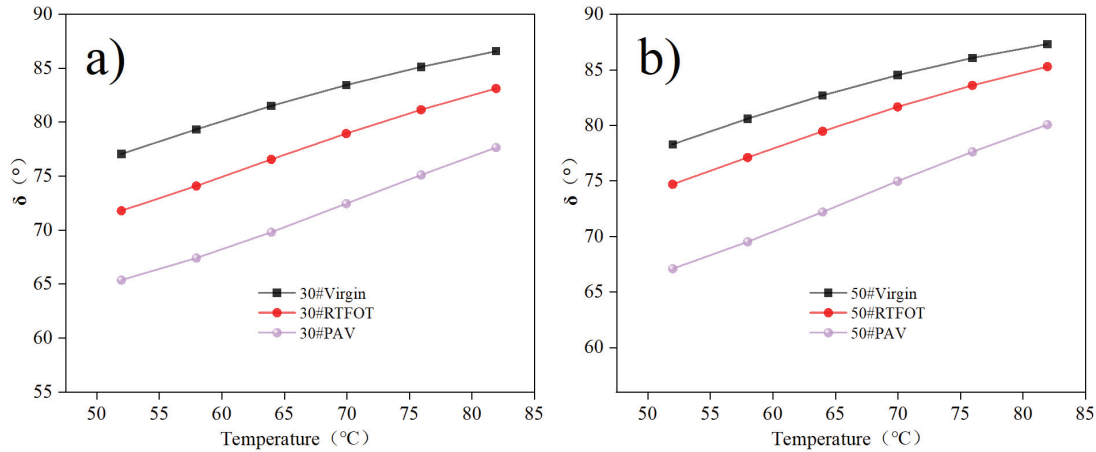
Figure 3: Phase angle under different aging conditions and different temperatures: (a) 30# asphalt; (b) 50# asphalt.
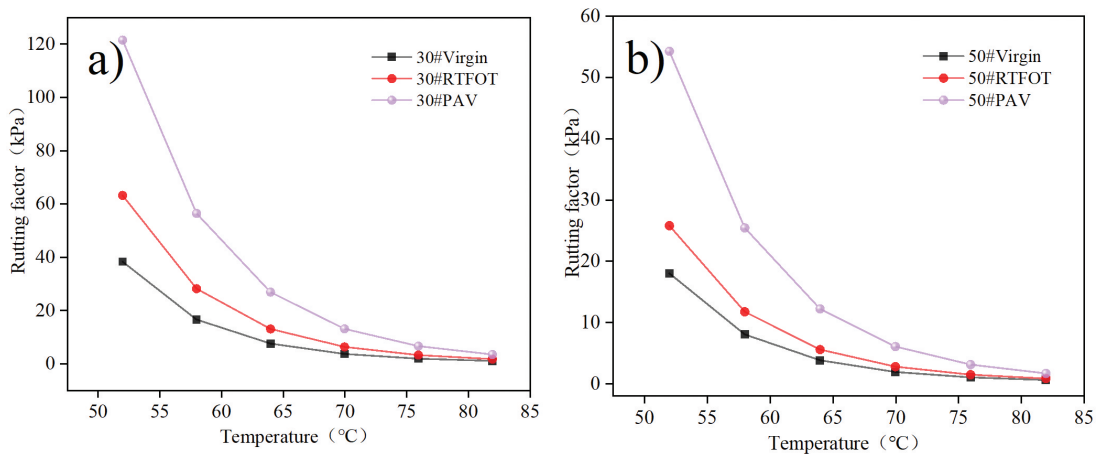

Figure 4: Rutting factor under different aging conditions and different temperatures: (a) 30# asphalt; (b) 50# asphalt.

ability under stress load. Conversely, a larger proportion of the elastic component corresponds to a better recovery deformation ability. Figure 3 presents the phase angle curves of the two types of low-grade asphalt before and after aging. It is observed that the phase angle of 50# asphalt is higher than that of 30#, indicating a higher viscosity ratio for the former. As the test temperature increases, the phase angle of both asphalt types gradually increases, signifying an increase in the proportion of viscous components and a decrease in the proportion of elastic components with rising temperature. In the temperature range of 52 °C to 82 °C, the growth rate of the phase angle gradually decreases. For example, the growth rate of the phase angle for 30# virgin asphalt within this temperature range is 2.95%, 2.75%, 2.37%, 2.03%, and 1.7%, respectively. Similar trends are observed for other asphalt samples, indicating that as aging progresses, the influence of temperature on the phase angle of asphalt diminishes, and the viscoelastic properties of asphalt tend to stabilize. Additionally, at the same temperature, the effect of PAV aging on the phase angle of asphalt is greater than that of RTFOT aging, consistent with the effect on the complex shear modulus.

3.1.3. Rutting factor

The combination of G* and δ provides a comprehensive evaluation of asphalt performance. The rutting factor, represented by G* / sinδ at the test temperature, characterizes the asphalt pavement's resistance to permanent deformation. A higher rutting factor indicates less flow deformation and better anti-rutting performance at the highest pavement design temperature. Figure 4 illustrates the rutting factors of the two asphalt types under different test conditions. Overall, the rutting factors decrease with increasing temperature, indicating reduced shear deformation resistance as temperature rises. This decrease is particularly pronounced in the range of 52 °C to 70 °C, signifying a rapid loss of elastic deformation ability in asphalt. However, as the temperature continues to rise, the curve gradually stabilizes, suggesting a similar level of anti-rutting ability. Notably, the rutting factor of 30# asphalt is consistently higher than that of 50# asphalt, indicating its stronger anti-rutting ability. Furthermore, the anti-rutting performance varies under different aging conditions. PAV aging has the greatest impact,
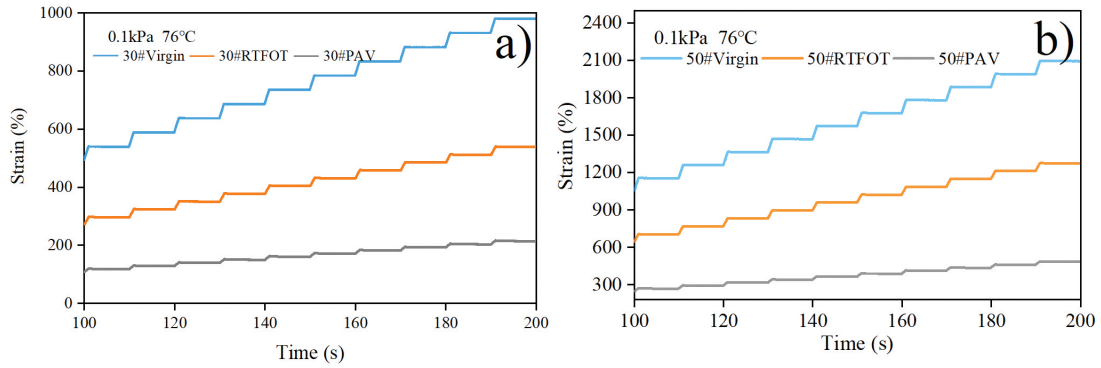
Figure 5: Creep recovery curves of asphalt under different aging conditions (0.1 kPa): (a) 30# asphalt; (b) 50# asphalt.

compared to RTFOT aging and UV aging. For instance, at 52 °C, the rutting factor of 30# asphalt increases by 65.18% and 218.06% after RTFOT and PAV aging, respectively, while the rutting factor of 50# asphalt increases by 43.55% and 202.6% under the same conditions. Long-term aging significantly enhances the rutting factor, indicating that aging improves the anti-rutting performance of low-grade asphalt. Some studies have shown that the rutting factor is not suitable for analyzing the rutting performance of asphalt [28, 29]. Therefore, this paper further uses the MSCR test to further analyze the high temperature rheological properties of low-grade asphalt.

3.2. MSCR TEST

3.2.1. Creep recovery curve

The MSCR test allows us to obtain the creep and recovery curves of asphalt at various stress levels and temperatures, enabling the calculation of the unrecoverable creep compliance and creep recovery rate. Figure 5 depicts the creep and recovery curves of the two asphalt samples at a temperature of 76 °C and a stress level of 0.1 kPa.

From Figure 5, it is evident that at the same stress level, the strain of 50# asphalt is considerably higher than that of 30# asphalt. Moreover, an increase in temperature results in an increase in asphalt strain, with higher temperatures exhibiting higher strain growth rates. Generally, each cycle of the creep curve exhibits a creep recovery stage. The virgin asphalt depicted in the Figure 5 displays smallest creep among the three asphalts, while the aged asphalt exhibits slight creep, particularly the PAV-aged asphalt, which demonstrates a more pronounced creep recovery stage. This indicates that aged low-grade asphalt exhibits some flow deformation characteristics at high temperatures. However, as aging progresses, asphalt strain decreases, and the creep recovery curve shifts downwards. The creep recovery curve of the PAV-aged asphalt is positioned at the bottom of the diagram, suggesting a significant reduction in asphalt strain under stress. This phenomenon indicates that aging leads to the "hardening" of the asphalt pavement, with a deeper degree of aging resulting in a more pronounced "hardening" effect. This is consistent with the results of JULAGANTI *et al.* [30].

3.2.2. Unrecoverable creep compliance

The unrecoverable creep compliance J_{nr} is a measure of asphalt's resistance to permanent deformation. A smaller J_{nr} value indicates a stronger ability to resist deformation and better high-temperature performance. Figure 6 illustrates the J_{nr} values of low-grade asphalt under various aging conditions, calculated at stress levels of 0.1 kPa and 3.2 kPa.

Figure 6 illustrates the behavior of the unrecoverable creep compliance J_{nr} for low-grade asphalt under different aging conditions at stress levels of 0.1 kPa and 3.2 kPa. Overall, at the same stress level, the J_{nr} of the asphalt increases with temperature. For example, under 0.1 kPa stress, the J_{nr} of 30# virgin asphalt increases from 12.299 kPa^{-1} at 52 °C to 853.664 kPa^{-1} at 82 °C, while the J_{nr} of 50# virgin asphalt increases from 35.082 kPa^{-1} to 1888.838 kPa^{-1} over the same temperature range. It is evident that the deformation resistance of 50# virgin asphalt is inferior to that of 30# asphalt. Notably, the J_{nr} exhibits significant changes in the high-temperature range, while it remains relatively stable at low temperatures. This indicates that high temperatures greatly affect the anti-deformation ability of asphalt. Moreover, after RTFOT aging, the J_{nr} values of both 30# and 50# asphalt increase, with 30# asphalt experiencing an increase of 495.949 kPa^{-1} under 0.1 kPa stress and 626.313 kPa^{-1} under 3.2 kPa stress from 52 °C to 82 °C. Similarly, the J_{nr} of 50# asphalt increases by 1127.674 kPa^{-1} and 1425.283 kPa^{-1} under the same temperature and stress conditions. These results highlight that the deformation resistance of 50# asphalt is inferior to that of 30# asphalt.
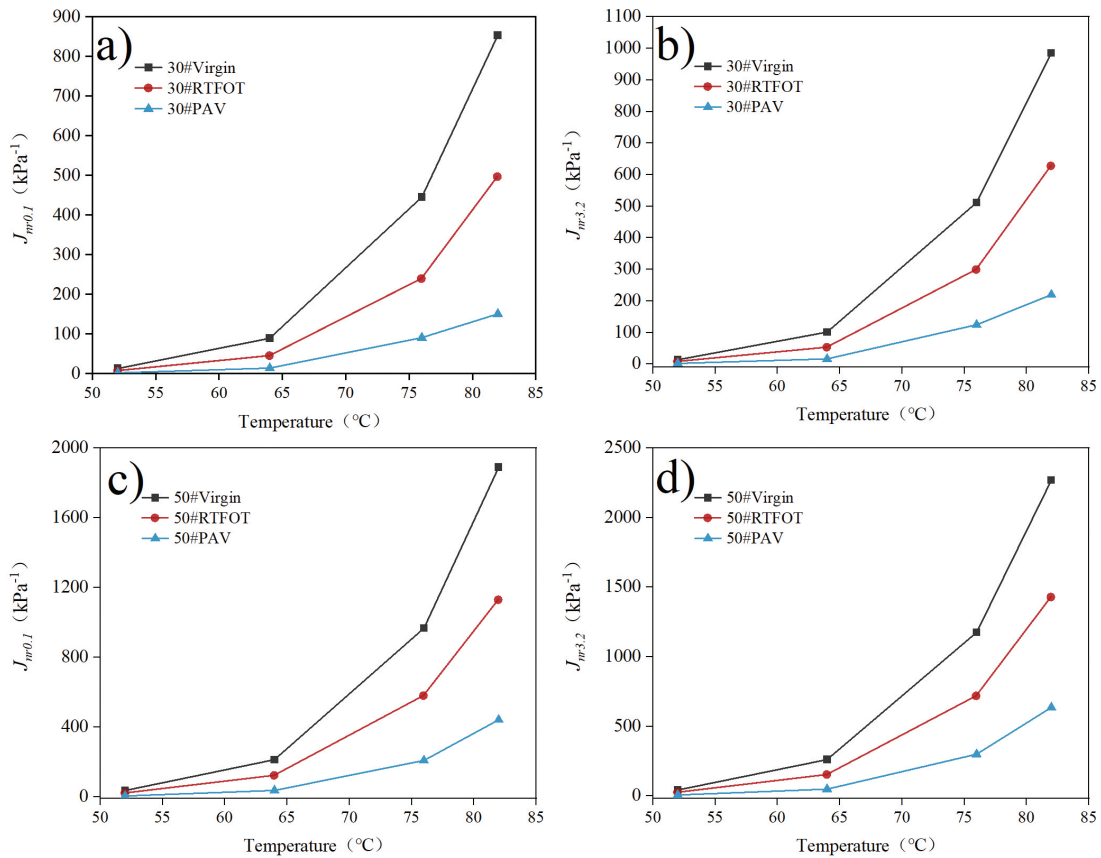
Figure 6: Unrecoverable creep compliance of asphalt under stress of 0.1 kPa and 3.2 kPa: (a) 30#asphalt, $J_{nr0.1}$; (b) 30#asphalt, $J_{nr3.2}$; (c) 50#asphalt, $J_{nr0.1}$; (d) 50#asphalt, $J_{nr3.2}$.

The stress level has an impact on the magnitude of the J_{nr} for virgin asphalt, with higher stress levels resulting in larger J_{nr} values compared to lower stress levels. This indicates that higher stress loads exerted on the asphalt lead to poorer anti-deformation ability, highlighting that the asphalt performs better under low stress conditions. Similarly, at the same stress level and temperature, the J_{nr} of the asphalt decreases after aging, which is consistent with the analysis results of LIU *et al.* [31]. For instance, at 0.1 kPa and 52 °C, the J_{nr} of 30# virgin asphalt decreases by 56.5% and 90.4% after RTFOT and PAV aging, respectively, while the J_{nr} of 50# virgin asphalt decreases by 50.8% and 88.8% under the same aging conditions. These findings demonstrate that aging reduces the J_{nr} of the asphalt, with a more pronounced reduction observed with higher degrees of aging. Moreover, upon comparing the J_{nr} creep curves of asphalt in Figure 6, it is apparent that the curve for aged asphalt shifts downwards, with the PAV aging curve located at the bottom of the figure. This indicates that PAV aging enhances the high-temperature deformation resistance of the asphalt, as reflected by its smaller irrecoverable creep compliance values.

3.2.3. Creep recovery rate

The creep recovery rate (R) is a measure of asphalt's ability to recover from deformation. A higher value indicates a stronger deformation recovery ability. Figure 7 presents the R of low-grade asphalt under various aging conditions, calculated at stress levels of 0.1 kPa and 3.2 kPa.

It is evident from Figure 7 that the R decreases as the temperature increases. This decrease is more pronounced in the lower temperature range (e.g., 52 °C to 70 °C), while it is relatively smaller in the higher temperature range. Particularly under a stress level of 3.2 kPa, the curve exhibits a gentler slope at higher temperatures, indicating a poorer creep recovery rate. Comparing the creep recovery rates under different stress levels, it is observed that asphalt exhibits lower creep recovery performance under higher stress levels. For instance, at a temperature of 64 °C, the creep recovery rate of 30# Virgin asphalt is 9.12% at 0.1 kPa stress, whereas it reduces to 3.03% at 3.2 kPa stress, indicating a 66.8% decrease in creep recovery performance. Similarly, at the same temperature, the creep recovery rate of 50# Virgin asphalt is 7.57% at 0.1 kPa stress, but it drops significantly to 0.077% at 3.2 kPa stress, representing a 98% reduction in creep recovery performance. In conclusion, high
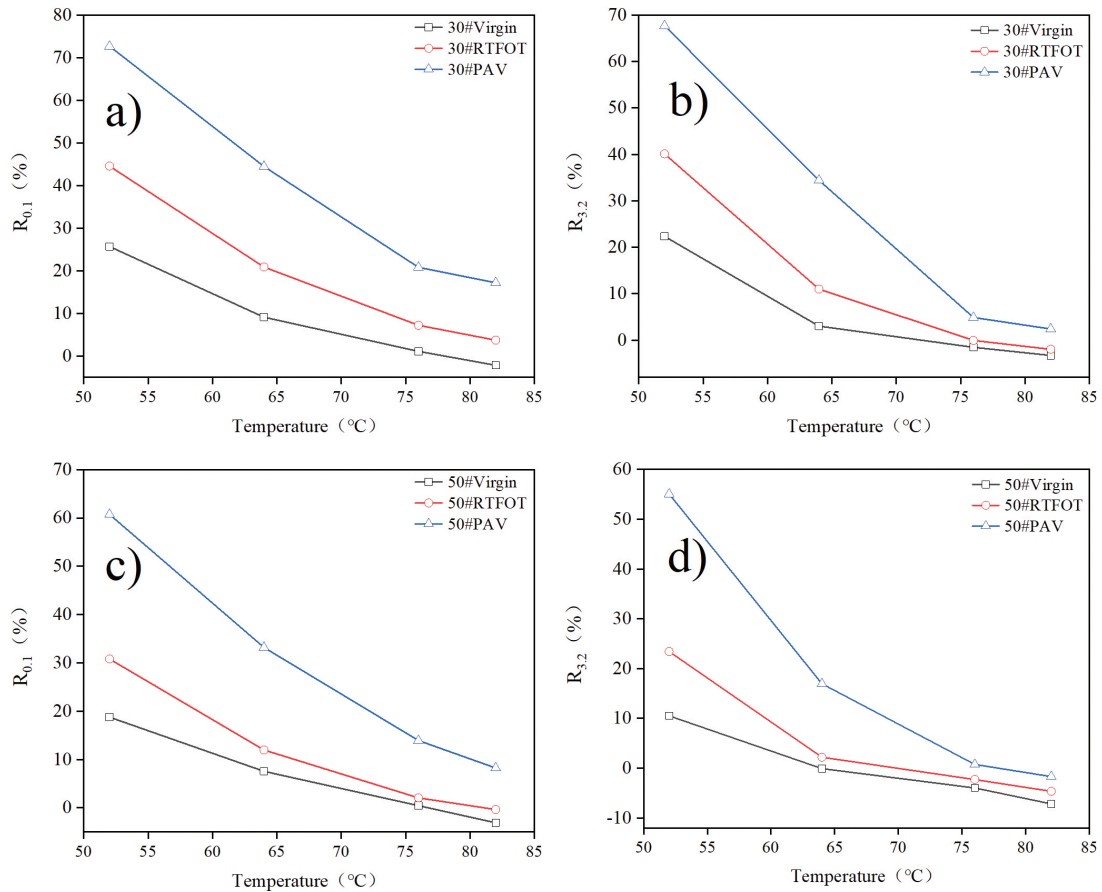
Figure 7: Creep recovery rate of asphalt under stress of 0.1 kPa and 3.2 kPa: (a) 30#asphalt, $R_{0.1}$; (b) 30#asphalt, $R_{3.2}$; (c) 50#asphalt, $R_{0.1}$; (d) 50#asphalt, $R_{3.2}$.

stress levels have a substantial impact on asphalt's creep performance, and 30# asphalt demonstrates superior creep recovery performance compared to 50#.

Under the same stress level and temperature condition, an increase in the aging degree of asphalt results in an increase in its creep recovery rate. Specifically, in the case of PAV aging, the curve is positioned at the upper part of the graph, indicating that aging facilitates the transition of asphalt from a viscous state to an elastic state. This transition leads to an increase in the elastic ratio and rigidity of the asphalt, thereby improving its creep recovery rate. Consequently, the asphalt becomes more elastic and structurally stable. ZHANG *et al.* [32] also showed the same trend in the MSCR study of six modified asphalts with multiple modifiers and different modifier contents. However, at 76 °C, the creep recovery rate of certain asphalt samples, such as 30# and 50# Virgin asphalt under 3.2 kPa stress, becomes less than zero. This suggests that the internal structure of the asphalt has been compromised, and its elastic properties have undergone significant changes. As a result, the deformation stability of the asphalt pavement is compromised, increasing the likelihood of cracks, deformations, and other pavement distresses.

3.2.4. The relative difference of irreversible creep compliance and the relative difference of creep recovery rate

In general, the stress sensitivity of asphalt can be characterized by two indices: the relative difference of unrecoverable creep compliance ($J_{nr\,diff}$) and the relative difference of creep recovery rate (R_{diff}). These indices provide insights into the nonlinear behavior of asphalt materials and the elastic stability of asphalt, respectively. A higher $J_{nr\,diff}$ value indicates a more pronounced nonlinear response of asphalt to varying stress levels, while a lower R_{diff} value signifies better elastic stability of the asphalt. The corresponding results are presented in Figure 8 and Table 3.

It is evident from Figure 8 that the $J_{nr\,diff}$ values of both virgin asphalts comply with the requirements of the AASHTO M 332-20 standard, which specifies a maximum $J_{nr\,diff}$ value of 75%. Overall, the $J_{nr\,diff}$ value of 30#
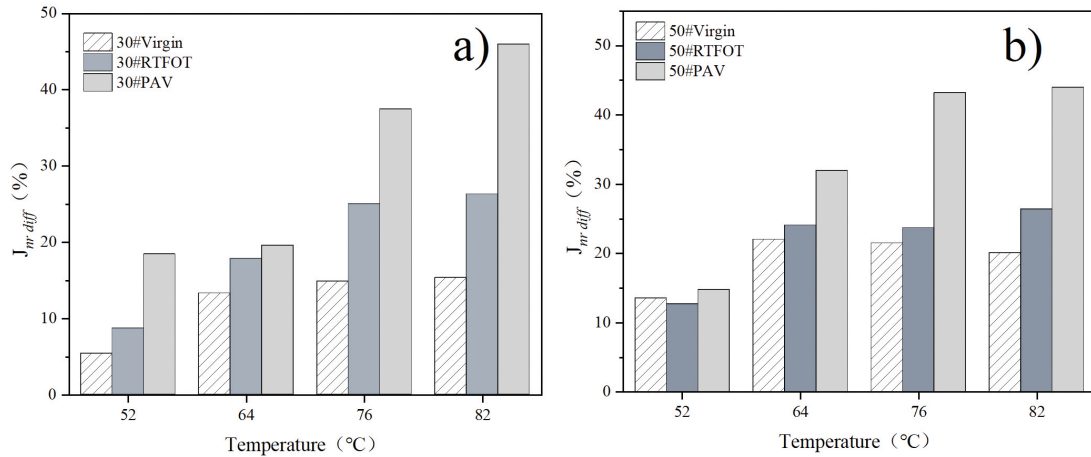
Figure 8: The relative difference of unrecoverable creep compliance of virgin asphalt: (a) 30#asphalt; (b) 50#asphalt.

Table 3: The relative difference of creep recovery rate (%).

ASPHALT	TEMPERATURE	VIRGIN	RTFOT	PAV
30#	52 °C	13.04	10.00	6.88
	64 °C	66.83	47.31	22.61
	76 °C	237.82	99.17	76.46
	82 °C	307.60	152.55	85.90
50#	52 °C	44.01	23.96	9.34
	64 °C	98.09	81.66	48.96
	76 °C	963.59	210.22	94.64
	82 °C	1193.28	694.27	120.51

asphalt is lower than that of 50# asphalt, indicating that 30# asphalt exhibits better resistance to stress changes and higher high temperature stability. However, for 30# asphalt, the $J_{nr\,diff}$ values after RTFOT at 76 °C and PAV at 82 °C are higher than those of 50# asphalt. Additionally, the $J_{nr\,diff}$ of 50# asphalt remains relatively stable after 76 °C, while the $J_{nr\,diff}$ of 30# asphalt continues to increase. This suggests that the aged 30# asphalt may have a higher temperature sensitivity compared to the aged 50# asphalt at higher temperatures.

From the observations in Table 3, it is evident that the R_{diff} values of asphalt increase as the temperature rises. This indicates that higher temperatures make the asphalt more sensitive to stress changes and further diminish its elastic recovery performance. Furthermore, as the aging degree of asphalt intensifies, the R_{diff} value gradually decreases. Notably, the R_{diff} value is the lowest for PAV aging, suggesting that the elastic recovery performance of asphalt is less influenced by stress after aging.

Overall, 30# asphalt exhibits better high temperature stability compared to 50# asphalt. It also demonstrates superior temperature sensitivity and elastic sensitivity when compared to 50# asphalt. It should be noted that as the temperature increases, the temperature sensitivity and elastic sensitivity of low-grade asphalt deteriorate. Additionally, prolonged aging time further diminishes the temperature sensitivity of low-grade asphalt while increasing its elastic sensitivity.

4. ROAD PERFORMANCE OF LOW-GRADE ASPHALT MIXTURE

4.1. Rutting resistance performance

In this study, the high temperature stability of low-grade asphalt mixture was assessed through rutting tests. The rutting tests were conducted on the optimized 30# and 50# low-grade asphalt mixtures at the recommended asphalt content. The results of the tests are presented in Figure 9. The tests were performed at a temperature of 60 °C to evaluate the rutting performance of the asphalt mixture under high temperature conditions. Additionally, to further investigate its performance, a rutting test was conducted at an elevated temperature of 70 °C. The dynamic stability parameter was used to assess the high temperature anti-rutting performance of the asphalt mixture, where higher values indicate better performance.
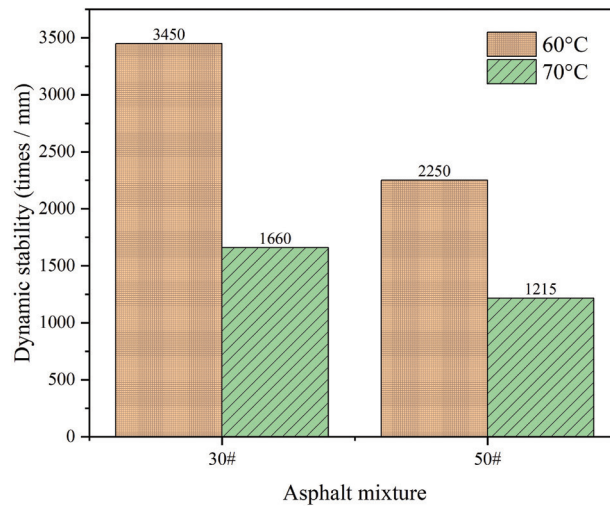
Figure 9: Asphalt dynamic stability results.

Table 4: Low temperature bending test results.

ASPHALT MIXTURE	BENDING STRENGTH (Mpa)	MAXIMUM BENDING STRAIN (µε)	BENDING STIFFNESS MODULUS (MPa)
30#	52 °C	13.04	6.88
	64 °C	66.83	22.61
	76 °C	237.82	76.46
	82 °C	307.60	85.90
50#	52 °C	44.01	9.34
	64 °C	98.09	48.96
	76 °C	963.59	94.64
	82 °C	1193.28	120.51

As depicted in Figure 9, both asphalt mixtures exhibit dynamic stability values exceeding 1000 times/mm, thereby satisfying the high temperature stability requirements for asphalt mixtures. Notably, the dynamic stability of the 30# asphalt mixture is notably higher than that of the 50# asphalt mixture. Specifically, at 60 °C, the dynamic stability of the 30# asphalt mixture is nearly double that of the 50# asphalt mixture. This finding indicates that the high temperature stability of the 30# asphalt mixture is significantly superior to that of the 50# asphalt mixture. Thus, lower-grade asphalt demonstrates improved high temperature stability. Furthermore, when the ambient temperature is raised to 70 °C, the dynamic stability of both asphalt mixtures decreases significantly, while maintaining a consistent trend with the results obtained at 60 °C.

4.2. Low-temperature stability

The low-temperature performance of different grade asphalt mixtures was assessed through the low-temperature trabecular bending test, and the results are presented in Table 4. It can be observed that the flexural strength of the 30# asphalt mixture is lower than that of the 50# asphalt mixture, and are lower than the commonly used asphalt mixture [33], indicating a weaker resistance to flexural load. The bending stiffness modulus refers to the resistance of asphalt mixture to deformation under bending action at low temperatures. It reflects the rigidity and deformation resistance of the asphalt mixture at low temperatures. Generally, the lower the bending stiffness modulus, the better the flexibility and deformation resistance of the asphalt mixture at low temperatures. The bending stiffness modulus of 50# asphalt is lower than that of 30# asphalt mixture, indicating that the 50# asphalt mixture has superior low-temperature resistance to bending and stretching. Similarly, the strain of the 30# asphalt mixture is smaller compared to the 50# asphalt mixture, suggesting a lesser capacity to withstand bending deformation. However, it is important to note that the evaluation of low-temperature behavior solely based on bending strain is limited. In practical applications, the low-temperature failure of asphalt mixtures typically occurs through creep fracture under continuous loads. The driving load experienced by the pavement is unlikely to replicate the effect of a single load that causes immediate pavement failure. Moreover, low-grade

asphalt mixtures are commonly used in the intermediate and lower layers of high-temperature regions, where the extreme low-temperature conditions are less severe compared to surface layers. Therefore, considering these factors, the risk of low-temperature cracking is minimal when utilizing 30# and 50# asphalt mixtures in the intermediate and lower layers of high-temperature areas.

5. CONCLUSIONS

The key findings and conclusions of this research are outlined below.

(1) The rheological properties of asphalt were assessed through DSR tests, both before and after aging. The findings indicate that as the asphalt label increases, the corresponding complex shear modulus decreases and the phase angle increases. Among the virgin asphalt samples, 30# asphalt demonstrates superior anti-rutting performance compared to 50#, SBS, and 70# virgin asphalt. Notably, 30# asphalt exhibits the highest resistance to deformation. Throughout the aging process, the rutting factor and fatigue factor of 30# asphalt are significantly higher than those of 50# asphalt.

(2) MSCR tests were conducted at temperatures of 52 °C, 64 °C, 72 °C, and 82 °C to examine the creep recovery behavior of the two low-grade asphalts under different temperature and aging conditions. The findings reveal that the strain of asphalt gradually increases with rising temperature, stress level, and stress duration. Moreover, the unrecoverable creep compliance of 50# asphalt is higher than that of 30#. Overall, low-grade asphalt exhibits relatively stable stress variations and demonstrates good high temperature stability.

(3) The high temperature stability and low temperature stability of low-grade asphalt mixture were evaluated. The findings indicate that the high temperature performance of 30# asphalt mixture surpasses that of 50# asphalt mixture. However, it displays lower flexural tensile strength and flexural tensile deformation ability at low temperatures compared to the 50# asphalt mixture. Therefore, low-grade asphalt mixture can be effectively utilized as the middle and lower surface layer in high temperature areas.

6. ACKNOWLEDGMENTS

7. BIBLIOGRAPHY

[1] XIA, Q.P., LI, Y.Y., XU, H.N., *et al.*, "Using phenol formaldehyde resin, hexamethylenetetramine and matrix asphalt to synthesize hard-grade asphalts for high-modulus asphalt concrete", *Sustainability*, v. 14, n. 23, pp. 15689, 2022. doi: http://dx.doi.org/10.3390/su142315689

[2] ZENG, G.D., WU, W.J., LI, J.C., *et al.*, "Comparative study on road performance of low-grade hard asphalt and mixture in China and France", *Coatings*, v. 12, n. 2, pp. 270, 2022. doi: http://dx.doi.org/10.3390/coatings12020270

[3] ZHOU, J., LI, J., LIU, G.Q., *et al.*, "Recycling aged asphalt using hard asphalt binder for hot-mixing recycled asphalt mixture", *Applied Sciences-basel*, v. 11, n. 12, pp. 5698, 2021. doi: http://dx.doi.org/10.3390/app11125698

[4] LI, M., ZENG, F., XU, R.G., *et al.*, "Study on compatibility and rheological properties of high-viscosity modified asphalt prepared from low-grade asphalt", *Materials (Basel)*, v. 12, n. 22, pp. 3776, 2019. doi: http://dx.doi.org/10.3390/ma12223776. PubMed PMID: 31744241

[5] TONG, Y.J., SHEN, B.X., LIU, J.C., *et al.*, "Preparation and evaluation of 30# hard grade asphalt", *Petroleum Science and Technology*, v. 35, n. 5, pp. 436–442, 2017. doi: http://dx.doi.org/10.1080/10916466.2016.1261161

[6] NASCIMENTO, F.C., GUIMARAES, A.C.R., CASTRO, C.D., "Comparative study on permanent deformation in asphalt mixtures from indirect tensile strength testing and laboratory wheel tracking", *Construction & Building Materials*, v. 305, pp. 124736, 2021. doi: http://dx.doi.org/10.1016/j.conbuildmat.2021.124736

[7] YUAN, D., JIANG, W., SHA, A., *et al.*, "Technology method and functional characteristics of road thermoelectric generator system based on seebeck effect", *Applied Energy*, v. 331, pp. 120459, 2023. doi: http://dx.doi.org/10.1016/j.apenergy.2022.120459

[8] GAO, Y.M., ZHANG, Y.Q., OMAIREY, E.L., *et al.*, "Influence of anti-ageing compounds on rheological properties of bitumen", *Journal of Cleaner Production*, v. 318, pp. 128559, 2021. doi: http://dx.doi.org/10.1016/j.jclepro.2021.128559

[9] HU, Y.P., XIA, W., XUE, Y., *et al.*, "Evaluating the ageing degrees of bitumen by rheological and chemical indices", *Road Materials and Pavement Design*, v. 24, n. 1, pp. 19–36, 2023. doi: http://dx.doi.org/10.1080/14680629.2023.2180289

[10] AZARHOOSH, A., KOOHMISHI, M., "Investigation of the rutting potential of asphalt binder and mixture modified by styrene-ethylene/propylene-styrene nanocomposite", *Construction & Building Materials*, v. 255, pp. 119363, 2020. doi: http://dx.doi.org/10.1016/j.conbuildmat.2020.119363

[11] DAS, A.K., SINGH, D., "Influence of nano size hydrated lime filler on rutting performance of asphalt mastic", *Road Materials and Pavement Design*, v. 22, n. 5, pp. 1023–1043, 2021. doi: http://dx.doi.org/10.1080/14680629.2019.1660208

[12] LIU, H.Q., ZEIADA, W., AL-KHATEEB, G.G., *et al.*, "Analysis of mscr test results for asphalt binders with improved accuracy", *Materials and Structures*, v. 54, n. 2, pp. 92, 2021. doi: http://dx.doi.org/10.1617/s11527-021-01691-0

[13] ZHANG, L., XING, C., GAO, F., *et al.*, "Using dsr and mscr tests to characterize high temperature performance of different rubber modified asphalt", *Construction & Building Materials*, v. 127, pp. 466–474, 2016. doi: http://dx.doi.org/10.1016/j.conbuildmat.2016.10.010

[14] JUDYCKI, J., JASKULA, P., DOLZYCKI, B., *et al.*, "Investigation of low-temperature cracking in newly constructed high-modulus asphalt concrete base course of a motorway pavement", *Road Materials and Pavement Design*, v. 16, n. sup1, pp. 362–388, 2015. doi: http://dx.doi.org/10.1080/14680629.2015.1029674

[15] KOMARAGIRI, S., FILONZI, A., MASAD, A., *et al.*, "Using the dynamic shear rheometer for low-temperature grading of asphalt binders", *Journal of Testing and Evaluation*, v. 50, n. 3, pp. 1622–1633, 2022. doi: http://dx.doi.org/10.1520/JTE20210277

[16] ESPERSSON, M., "Effect in the high modulus asphalt concrete with the temperature", *Construction & Building Materials*, v. 71, pp. 638–643, 2014. doi: http://dx.doi.org/10.1016/j.conbuildmat.2014.08.088

[17] LOPEZ-MONTERO, T., MANOSA, J., MIRO, R., *et al.*, "Sustainable asphalt mixtures by partial replacement of fine aggregates with low-grade magnesium carbonate by-product", *Case Studies in Construction Materials*, v. 18, pp. e01705, 2023. doi: http://dx.doi.org/10.1016/j.cscm.2022.e01705

[18] BARRA, B.S., MOMM, L., PEREZ, Y.G., *et al.*, "A new dynamic apparatus for asphalt mix fatigue and stiffness modulus: development, validation and numerical simulations", *Matéria (Rio de Janeiro)*, v. 27, n. 1, pp. e13130, 2022. doi: http://dx.doi.org/10.1590/s1517-707620220001.1330

[19] ZHANG, F., CAO, Y., SHA, A., *et al.*, "Characterization of asphalt mixture using X-ray computed tomography scan technique after freeze-thaw cycle and microwave heating", *Construction & Building Materials*, v. 346, pp. 128435, 2022. doi: http://dx.doi.org/10.1016/j.conbuildmat.2022.128435

[20] ZHANG, F., CAO, Y., SHA, A., *et al.* "Mechanism, rheology and self-healing properties of carbon nanotube modified asphalt", *Construction and Building Materials*, v. 346, pp. 128431, 2022. doi: http://dx.doi.org/10.1016/j.conbuildmat.2022.128431

[21] SHA, A., LIU, Z., JIANG, W., *et al.*, "Advances and development trends in eco-friendly pavements", *Journal of Road Engineering*, v. 1, pp. 1–42, 2021. doi: http://dx.doi.org/10.1016/j.jreng.2021.12.002

[22] JIANG, W., YUAN, D.D., SHAN, J.H., *et al.*, "Experimental study of the performance of porous ultra-thin asphalt overlay", *The International Journal of Pavement Engineering*, v. 23, n. 6, pp. 2049–2061, 2022. doi: http://dx.doi.org/10.1080/10298436.2020.1837826

[23] SEDTHAYUTTHAPHONG, N., JITSANGIAM, P., NIKRAZ, H., *et al.*, "The influence of a field-aged asphalt binder and aggregates on the skid resistance of recycled hot mix asphalt", *Sustainability*, v. 13, n. 19, pp. 10938, 2021. doi: http://dx.doi.org/10.3390/su131910938

[24] ZHEN, T., KANG, X.X., LIU, J.Y., *et al.*, "Multiscale evaluation of asphalt aging behaviour: a review", *Sustainability*, v. 15, n. 4, pp. 2953, 2023. doi: http://dx.doi.org/10.3390/su15042953

[25] XU, J., MA, B., MAO, W., *et al.*, "Review of interfacial adhesion between asphalt and aggregate based on molecular dynamics", *Construction & Building Materials*, v. 362, pp. 129642, 2023. doi: http://dx.doi.org/10.1016/j.conbuildmat.2022.129642

[26] YANG, E., MA, B., LI, A., *et al*., "Effect of short-term aging on high temperature performance of expansion joint binder", *Municipal Engineering Technology*, v. 40, n. 5, pp. 181–188, 2022.

[27] MITTAL, A., ARORA, K., KUMAR, G., *et al*., "Comparative studies on performance of bituminous mixes containing laboratory developed hard grade bitumen", *Advances in Civil Engineering Materials*, v. 7, n. 2, pp. 92–104, 2018. doi: http://dx.doi.org/10.1520/ACEM20170039

[28] HAMID, A., BAAJ, H., EL-HAKIM, M., "Rutting behaviour of geopolymer and styrene butadiene styrene-modified asphalt binder", *Polymers*, v. 14, n. 14, pp. 2780, 2022. doi: http://dx.doi.org/10.3390/polym14142780. PubMed PMID: 35890556

[29] JAMSHIDI, A., GOLCHIN, B., HAMZAH, M.O., *et al*., "Selection of type of warm mix asphalt additive based on the rheological properties of asphalt binders", *Journal of Cleaner Production*, v. 100, pp. 89–106, 2015. doi: http://dx.doi.org/10.1016/j.jclepro.2015.03.036

[30] JULAGANTI, A., CHOUDHARY, R., KUMAR, A., "Permanent deformation characteristics of warm asphalt binders under reduced aging conditions", *KSCE Journal of Civil Engineering*, v. 23, n. 1, pp. 160–172, 2018. doi: http://dx.doi.org/10.1007/s12205-017-1903-0

[31] LIU, H., ZEIADA, W., AL-KHATEEB, G.G., *et al*., "Use of the multiple stress creep recovery (mscr) test to characterize the rutting potential of asphalt binders: a literature review", *Construction & Building Materials*, v. 269, pp. 121320, 2021. doi: http://dx.doi.org/10.1016/j.conbuildmat.2020.121320

[32] ZHANG, W., MA, T., XU, G., *et al*., "Fatigue resistance evaluation of modified asphalt using a multiple stress creep and recovery (mscr) test", *Applied Sciences (Basel, Switzerland)*, v. 8, n. 3, pp. 417, 2018. doi: http://dx.doi.org/10.3390/app8030417

[33] WANG, T., XIAO, F.P., AMIRKHANIAN, S., *et al*., "A review on low temperature performances of rubberized asphalt materials", *Construction & Building Materials*, v. 145, pp. 483–505, 2017. doi: http://dx.doi.org/10.1016/j.conbuildmat.2017.04.031